Identification of clinical and molecular features of recurrent serous borderline ovarian tumour

Ziyang Lu,[a,1] Fanghe Lin,[b,1] Tao Li,[c,1] Jinhui Wang,[a] Cenxi Liu,[a] Guangxing Lu,[a] Bin Li,[a] MingPei Pan,[a] Shaohua Fan,[a] Junqiu Yue,[d] He Huang,[a] Jia Song,[e]* Chao Gu,[a]* and Jin Li[a,f]**

[a]State Key Laboratory of Genetic Engineering, School of Life Sciences, Human Phenome Institute, Institute of Metabolism and Integrative Biology, Obstetrics and Gynecology Hospital of Fudan University, Fudan University, Shanghai 200438, China
[b]State Key Laboratory for Physical Chemistry of Solid Surfaces, Key Laboratory for Chemical Biology of Fujian Province, Key Laboratory of Analytical Chemistry, Department of Chemical Biology, College of Chemistry and Chemical Engineering, Xiamen University, Xiamen 361005, China
[c]Department of Obstetrics and Gynecology, Shandong Provincial Hospital Affiliated to Shandong First Medical University, Jinan, Shandong 250021, China
[d]Department of Pathology, Hubei Cancer Hospital, Tongji Medical College, Huazhong University of Science and Technology, Wuhan, Hubei 430079, China
[e]Institute of Molecular Medicine, School of Medicine, Renji Hospital, Shanghai Jiao Tong University, Shanghai 200127, China
[f]Institute of Cell Biology and Biophysics, Leibniz University Hannover, Hanover, Germany

Summary

Background Serous borderline ovarian tumour (SBOT) is the most common type of BOT. Fertility sparing surgery (FSS) is an option for patients with SBOT, though it may increase the risk of recurrence. The clinical and molecular features of its recurrence are important and need to be investigated in detail.

Methods An internal cohort of 319 patients with SBOT was collected from Aug 1, 2009 to July 31, 2019 from the Obstetrics and Gynecology Hospital of Fudan University in China. An external cohort of 100 patients with SBOT was collected from Aug 1, 2009 to Nov 30, 2019 from the Shandong Provincial Hospital in China. The risk factors for the recurrence were identified by multivariate cox analysis. Several computational methods were tested to establish a prediction tool for recurrence. Whole genome sequencing, RNA-seq, metabolomics and lipidomics were used to understand the molecular characteristics of the recurrence of SBOT.

Findings Five factors were significantly correlated with SBOT recurrence in a Han population: micropapillary pattern, advanced stage, FSS, microinvasion, and lymph node invasion. A random forest-based online recurrence prediction tool was established and validated using an internal cohort and an independent external cohort for patients with SBOT. The multi-omics analysis on the original SBOT samples revealed that recurrence is related to metabolic regulation of immunological suppression.

Interpretation Our study identified several important clinical and molecular features of recurrent SBOT. The prediction tool we established could help physicians to estimate the prognosis of patients with SBOT. These findings will contribute to the development of personalised and targeted therapies to improve prognosis.

Funding JL was funded by MOST 2020YFA0803600, 2018YFA0801300, NSFC 32071138, and SKLGE-2118 to Jin Li; JY was funded by the Initial Project for Young and Middle-aged Medical Talents of Wuhan City, Hubei Province ([2014] 41); HH was funded by MOST 2019YFA0801900 and 2020YF1402600 to He Huang; JS was funded by NSFC 22,104,080; CG was funded by Natural Science Foundation of Shanghai 20ZR1408800 and NSFC82171633; BL was funded by Natural Science Foundation of Shanghai 19ZR1406800.

Copyright © 2022 The Author(s). Published by Elsevier Ltd. This is an open access article under the CC BY-NC-ND license (http://creativecommons.org/licenses/by-nc-nd/4.0/)

Keywords: SBOT; Prediction model; Immunological suppression

eClinicalMedicine 2022;46: 101377
Published online xxx
https://doi.org/10.1016/j.eclinm.2022.101377

*Corresponding authors.
**Corresponding author at: State Key Laboratory of Genetic Engineering, School of Life Sciences, Human Phenome Institute, Institute of Metabolism and Integrative Biology, Obstetrics and Gynecology Hospital of Fudan University, Fudan University, Shanghai 200438, China.
E-mail addresses: songjiajia2010@shsmu.edu.cn (J. Song), chaogu@fudan.edu.cn (C. Gu), li_jin_lifescience@fudan.edu.cn (J. Li).

[1] These authors contributed equally in this work.

Research in context

Evidence before this study

Serous borderline ovarian tumour (SBOT) is a type of rare neoplasm that features atypical epithelial cell proliferation in the ovary. We searched PubMed to identify articles published until Dec 31, 2021 using the search key words "serous borderline ovarian tumors" AND "recurrence". The largest study of the Chinese population involved 101 patients and the largest study worldwide involved 1026 patients, but the prediction tools for SBOT recurrence were absent.

Added value of this study

Based on a cohort from the Obstetrics and Gynecology Hospital of Fudan University, we retrospectively retrieved complete clinical information of 319 patients with SBOT from 2009 to 2019. We discovered several independent recurrence-related factors and established a random forest-based model for recurrence prediction. Furthermore, the immunological suppression features associated with recurrent SBOT and its potential metabolic mechanism were identified by multi-omics assay on the original SBOT samples.

Implications of all the available evidence

To improve the efficacy of therapeutic treatment of SBOT, it is important to identify disease features that are correlated with recurrence. With a large SBOT cohort in a Han population, we discovered five factors related to recurrence. The identification between microinvasion or lymph node invasion and recurrence suggested more detailed report of pathology assessment for SBOT is required.

Introduction

Borderline ovarian tumour (BOT) is a type of rare neoplasm, without stromal invasion, that features atypical epithelial cell proliferation in ovary. In comparison to malignant ovarian tumours, patients with BOT tend to be much younger and have better prognosis.[1] The overall 5-year survival rate of patients with BOT in all stages is higher than 96%.[2] Serous borderline ovarian tumor (SBOT) is the most common type of BOT, which accounts for 50% of all BOT patients.[3] Despite its favorable prognosis, stage II or higher SBOT may still progress as low-grade serous carcinoma (LGSC).[4] Therefore, surgical removal of the tumor is considered as the first-line therapy for SBOT.

However, radical hysterectomy may not be the option for many patients with SBOT who are at reproductive age and wish for future fertility. Based on guidelines from the National Comprehensive Cancer Network (NCCN) and the results of several clinical studies, fertility sparing surgery (FSS) is an option for patients with SBOT.[5–7] The major issue with opting for FSS is the increased risk of tumor recurrence, which happens in 25.0–56.4% of patients with SBOT in the literature.[8–11] If the physicians for the patients with SBOT can estimate the risk of recurrence before surgery, it is possible to more carefully choose the best type of surgery and follow-up plan for specific patients.

Unfortunately, most of the clinical studies focused on the recurrence of SBOT have been conducted on relatively small patient cohorts with only short time periods of follow-up.[12,13] So far, the largest SBOT study was conducted on 1026 Denmark patients' clinical data.[14] For a Chinese population, the largest study involved only 101 patients with 12 patients (11.9%) developing tumor recurrence over a follow-up interval of 7 years.[15] Compared to the number of epidemiology studies, studies about the molecular features of SBOT are far more limited. These studies mostly focus on genomic mutations found in a small number of patients, based on assays with limited resolution and throughput.[16,17] There is a lack of systemic investigation on how SBOT features relate to genomics, transcriptomics, metabolites, and lipids. Performing such studies is important since identifying molecular features associated with SBOT recurrence may unveil targetable mechanisms to help promote the development of new therapeutics.

We hypothesised that studies on a large cohort for a long follow-up interval, with the employment of advanced computational and experimental methods, may identify important features of recurrent SBOT. Based on a cohort from the Obstetrics and Gynecology Hospital of Fudan University, we retrospectively retrieved complete clinical information of 319 patients with SBOT with 59 recurrences from 2009 to 2019. We discovered several independent recurrence-related factors, including microinvasion, lymph node invasion, and the type of FSS used in this cohorts. A random forest-based model for recurrence prediction successfully predicted reoccurrence in the internal cohort for this study (Area Under Curve of 0.999). Notably, this model also predicted recurrence accurately when used on an independent SBOT cohort containing 83 patients and 24 recurrences, with AUC of 0.817. Furthermore, the immunological suppression features associated with recurrent SBOT and its potential metabolic mechanism were identified by multi-omics assay on the original SBOT samples.

Methods

Patient recruitment

The internal cohort involved 321 patients that underwent surgeries for primary or post-relapse serous

borderline ovarian tumor from Aug 1, 2009 to July 31, 2019 from the Obstetrics and Gynecology Hospital of Fudan University in China. Their pathology results were reconfirmed blindly by two pathologists. We excluded two patients who were diagnosed with SBOT alongside invasive implantation, which should be treated as low-grade serous carcinoma according to the 2020 World Health Organization (WHO) Classification of Tumors of Female Reproductive Organs. The International Federation of Gynecology and Obstetrics 2014 criteria (FIGO 2014) was used for tumor staging. The external cohort with 100 patients who were diagnosed as SBOT after surgery was collected from Aug 1, 2009 to Nov 30, 2019 from the Shandong Provincial Hospital in China. The patients from these two cohorts come from 23 of 31 provinces in China. Our study was approved by the Ethics Committee of the Obstetrics and Gynecology Hospital of Fudan University (OBGYN 2019-70). All the participants provided written informed consent to take part in the study.

The collection of clinical information

Patients' basic information, such as medical files and follow-up data, was collected by two researchers. Patients who were younger than 40 years old or nulliparous were provided the option of fertility preservation for either initial treatment or recurrent surgery. FSS was used to preserve the uterus and at least one side of the ovaries, which included unilateral ovarian cystectomy (UOC), unilateral salpingo-oophorectomy (USO), bilateral ovarian cystectomy (BOC), and unilateral salpingo-oophorectomy plus contralateral ovarian wedge resection (USO+CWR). For the patients without fertility desire, total hysterectomy and bilateral salpingo-oophorectomy (TH+BSO) were suggested. Additional surgical steps were chosen selectively: removal of the pelvic lesions, multiple biopsies of the peritoneum, omentectomy, and lymphadenectomy. If SBOT tumor was unilateral, tumor size was defined as the maximum tumor diameter, or if tumors were bilateral, it was defined as the sum of bilateral tumors' diameters. Based on the National Comprehensive Cancer Network (NCCN) guideline, standard cytoreductive surgery includes the removal of the macroscopic lesions, peritoneal biopsy, peritoneal washings and omentectomy.[18] Incomplete surgery was defined as losing of any standard steps for surgery.

Patients attended follow-up appointments every 3 months during the first year, every 6 months during the second year, and every 12 months thereafter. The following information was collected: recurrence status, physical examination findings, tumor markers, ultrasound imaging, and magnetic resonance imaging (MRI) findings. Recurrence referred to discovering serous borderline lesion or low-grade serous carcinoma proven by surgery or highly suspicious pelvic mass on MRI test with elevated Carbohydrate Antigen 125 (CA125). Progression free survival time was the time interval between the primary operation and radiographic discovery of recurrence.

Data processing and model

Patient data from a total of 319 patients was included in the internal cohort, which contained 28 clinical indicators, including demographic characteristics, fertility status, clinical information, lab tests, surgical status, and pathological information. After filtering out 48 samples due to missing recurrence/non-recurrence labels, 271 samples consisting of 59 recurrences were used for the following analyses. To correct the class-imbalance, the information from 59 recurrent samples were randomly oversampled to expand the recurrence sample sets. The sensitivity analysis result of 'oversampling-method' was show in **Supplementary Figure 1A**. Ultimately, 424 samples consisting of 212 recurrence and 212 non-recurrence samples were available to build our prediction model. To validate the prediction model on an external data set containing 100 samples, the same 'label filtering' operation was performed and 83 samples were retained. Then, to handle the missing values of different clinical indicators, we performed data imputation using the missForest function from the R package "missForest" on both the internal and the external data sets to ensure smooth development of the subsequent training and prediction processes. The top three missing indicators are HE4 (39.83% of all the missing values), Carbohydrate Antigen199 (CA199, 12.33%) and aspartate aminotransferase (AST, 8.3%). The results of sensitivity analysis for "missForest" by artificially losing 1 −8% of the data at random were shown at **Supplementary Figure 1B**. The sensitivity analysis on imputation of top three missing indicators was presented at **Supplementary Figure 1C**.

Two-thirds of the internal cohort was then randomly selected and treated as a training set to construct a Random Forest Regressor for recurrent prediction. The other 1/3 were used as the internal test set. During the training, we executed tests more than 20 times to ensure that the model was stable in predicting recurrence. We evaluated the performance of the model by applying it to the remaining one-third of patients in the internal data set and the external data set. Since we used a regression model, which gave a continuous prediction value between 0 and 1, a threshold value is required to meet a binary classification problem. According to the performance of the best model on both internal and external data sets, 0.5 was finally selected as the threshold. Thus, patients with predicted values > 0.5 are regarded as the ones who will get a high probability of being suffered from recurrence. This model was saved and used as the predictor on the website.

Considering that medical workers have certain difficulties in collecting data on all 28 clinical indicators, a model with fewer required indicators should be established to adapt to more situations. We quantified the importance of the indicators (known as variables) with a mean decrease Gini score. Variables with higher mean decrease Gini scores play more important roles in the prediction. The curve of ranked mean decrease Gini showed that the change of mean decrease Gini of the variables after the seventh became flat. We then screened out seven variables based on the mean decrease Gini scores to train a simplified model. The all-indicator predictor and the simplified one are both available on the website (http://117.25.169.110:1030/).

Comparison with other methods

Here, we tested several popular supervised methods to clarify the performance of different algorithms on our data set. These algorithms included lightGBM, XGboost, gcForest, and Random Forest Regressor. For each method, we fed training set data into the model and performed parameters tuning over 20 times to maximize the Area Under Curve (AUC)-Receiver Operating Characteristic (ROC). In the internal cohort, these models achieved the following AUCs: lightGBM:0.950, XGboost: 0.971, gcForest:0.986, and Random Forest Regressor:0.999. The Random Forest Regressor showed best ability with our dataset for predicting recurrence. Information about the accuracy and parameters of each algorithm was summarized in **Supplementary Table 2.**

Online tool establishment

The training models are available at http://117.25.169.110:1030/. This website was developed based on Gin web framework with pages designed with BootStrap.

Survival analyses

The effects of selected clinical indicators on SBOT recurrence rates were tested by univariate cox analysis using Kaplan-Meier methods. Multivariate cox analysis was implemented to appraise the relationship between the risk of recurrence and clinical variables which showed significant correlation in the univariate analysis. Considering that there was only one stage 4 patient sample and its non-recurrence outcome may affect the hazard ratio result of the 'stage' indicator, we deleted it before the cox analysis. Ultimately, we presented a survival curve with features that were significantly related to recurrence. All analyses in this section were performed with the python package 'lifelines (v0.26.3)' (Davidson-Pilon, Cameron. (2021)) in Python.

Whole genome sequencing

Approximately 50–100 mg of tissue was cut up into pieces and added to a preheated (56 °C) 2 mL EP tube with 1 mL lysis buffer (100 μL 20 mg/mL Proteinase K and 100 μL 20%SDS) and incubated at 56 °C for 60~120 min. The tube was centrifuged at 18,213×*g* for 10 min and then cooled to room temperature before supernatant collection. The supernatant was transferred to a new 2.0 mL tube, adding equal volume of supernatant and Phenol/Chloroform/isoamylalcohol (25: 24:1), and centrifuged at 18,213×*g* for 10 min. The supernatant was added to a new 1.5 mL tube and 2/3th of the supernatant volume of isopropyl alcohol was added (add 1/10th volume of 3 M sodium acetate if necessary), and then the tube was inverted at least 3 times and placed at −20 °C for 2 h for precipitation. To remove the supernatant, the tube was centrifuged at 18,213×*g* for 10 min, which resulted in DNA pelleting. The pellet was then washed with 1 mL 75% ethanol. The pellet was resuspended by centrifuging at 18,213×*g* for 5 min at room temperature and the supernatant was removed. We then air-dried the DNA pellet in a biosafety cabinet for a few minutes and added 25~100 μL of TE Buffer to dissolve the DNA pellet. The DNA's concentration was detected by Qubit Fluorometer. Both sample integrity and purity were detected by Agarose Gel Electrophoresis. We randomly fragmented 1 μg of genomic DNA using Covaris, and the fragmented DNA was selected by Agencourt AMPure XP-Medium kit for an average size of 200–400 bp. The selected fragments underwent through end-repair, 3′ adenylated, adapters-ligation, and PCR amplifying, and the products were recovered using the AxyPrep Mag PCR clean up Kit. The double stranded PCR products were heat denatured and circularized by the splint oligo sequence. The single stranded circularized DNAs (ssCir DNA) were formatted as the final library and quantified by quality control (QC). The qualified libraries were sequenced on a BGISEQ-500 platform (BGI-Shenzhen, China). The raw sequencing data was processed using the following steps: (1) Removing reads containing the sequencing adapter; (2) Removing reads whose low-quality base ratio (base quality less than or equal to 5) is more than 50%; (3) Removing reads whose unknown base ('N' base) ratio is more than 10%. Statistical analysis of data and downstream bioinformatics analysis were performed on this filtered, high-quality data, referred to as the clean data.

The clean data were mapped to the human reference genome (GRCh38) using BWA version 0.7.17-r1188 with MEM mode. We conducted SNP calling using GATK v4.1.7.0 toolkit and annotated the functional impacts of the variants with Annovar version 2019-10-24. Using Vcftools (version 0.1.16), we calculated the Fst statistic (parameter –fst), which is widely used in population genetics, to identify the variants that are group-specific. When a variant is shared by all the individuals in a case group but cannot be found in any

individuals of the control group or vice versa, the Fst of this variant is 1.

RNA-seq analysis

Total RNA was extracted from tissues by using TRIzol reagent (Invitrogen). Sequencing libraries were generated using NEBNext® UltraTM RNA Library Prep Kit for Illumina® (NEB, USA) and index codes were added to attribute sequences to each sample. Briefly, mRNA was purified from total RNA using poly-T oligo-attached magnetic beads. Fragmentation was carried out using divalent cations under elevated temperature in NEBNext First Strand Synthesis Reaction Buffer (5X). First strand cDNA was synthesized using random hexamer primers and M-MuLV Reverse Transcriptase (RNase H-). Second strand cDNA synthesis was subsequently performed using DNA Polymerase I and RNase H. Remaining overhangs were converted into blunt ends via exonuclease/polymerase activities. After adenylation of 3′ ends of DNA fragments, NEBNext Adaptors with hairpin loop structure were ligated to prepare for hybridization. In order to select cDNA fragments with 250~300 bp, the library fragments were purified using the AMPure XP system (Beckman Coulter, Beverly, USA). Then 3 μL of USER Enzyme (NEB, USA) was used with size-selected, adaptor-ligated cDNA at 37 °C for 15 min, followed by 5 min at 95 °C before PCR. Then PCR was performed with Phusion High-Fidelity DNA polymerase, Universal PCR primers, and Index (X) Primer. At last, PCR products were purified (AMPure XP system) and library quality was assessed on the Agilent Bioanalyzer 2100 system. The clustering of the index-coded samples was performed on a cBot Cluster Generation System using TruSeq PE Cluster Kit v3-cBot-HS (Illumia). After cluster generation, the library preparations were sequenced on an Illumina Hiseq platform and 125–150 bp paired-end reads were generated.

Raw data of fastq format were firstly processed through in-house perl scripts. In this step, clean data were obtained by removing reads containing adapter and trimming low qulity base with Trimmomatic.[19] Index of the reference genome was built using Hisat2 and paired-end clean reads were aligned to the reference genome using Hisat2. StringTie was applied to the bam file for expression quantification and the RNA-seq count data was obtained. Finally, differential expression analysis of two groups was performed using the DESeq2 R package.[20]

Quantitative RT-PCR

TRIzol (Thermo Fisher) was used for total tissue and RNA isolation. Extracted RNA (500 ng) was converted into cDNA using the PrimeScript™ RT reagent Kit (Takara). Quantitative RT-PCR (qRT-PCR) was performed using an Applied Biosystems QuantStudio 5 and SYBR Green PCR Master Mix (Applied Biosystems). Fold change was determined by comparing target gene expression with the reference gene *36B4*. The sequence of primers is presented in **Supplementary Table 1**.

Hydrophilic metabolite extraction

Tissue samples were homogenized at −20 °C for 1.5 h. Methanol: water (*v:v*, 80:20) was pre-chilled at −80 °C overnight, and 4 mL was added to the tissue sample homogenate. The homogenate was then incubated at −80 °C for 20 min and decanted to a 15 mL centrifuge tube. The homogenate was centrifuged at 4 °C at 4000 x g for 10 min, and the supernatant was then collected in another 15 mL centrifuge tube. 500 μL of pre-chilled 80% methanol was added to the 15 mL centrifuge tube which contained the tissue homogenate, and after 1 min of vortexing, the tissue homogenate was centrifuged at 4 °C at 4000 x *g* for 10 min again. Approximately 500 μL of supernatant was added to the ~4 mL of supernatant in a new 15 mL centrifuge tube. The 4.5 mL supernatant was split into three portions (3 × 1.5 mL microcentrifuge tubes). The 80% methanol extracted metabolites were then dried using a SpeedVac (LABCONCO Refrigerated CentriVap Concentrator) and stored at −80 °C before MS analysis.

Tissue lipid extraction

A tissue sample was added to 200 μL of water and 500 μL of methanol and homogenized using the same approach as in the hydrophilic metabolite extraction above. The homogenate was supplemented with 500 μL more methanol and decanted into a clean glass centrifuge tube. Five milliliters of MTBE were then added to the glass centrifuge tube and vortexed for one min. The glass centrifuge tube containing the homogenate was rocked on a shaker for one hour at room temperature. 1.25 mL of water was then added to the glass centrifuge tube followed by another minute of vortexing. The homogenate was centrifuged at 4 °C at 1000 x *g* for 10 min and two- phase layers could be observed in the glass centrifuge tube. Four milliliters of the top phase supernatant were collected and dried under a stream of nitrogen. The extracted lipid sample was stored at −80 °C before MS analysis. The detailed protocols for lipid and metabolites extraction have been published.[21]

Targeted metabolomics

The aqueous metabolites were reconstituted using 100 μL acetonitrile: water (*v:v* 50:50). Then, 5 μL of the reconstituted sample was injected into the Liquid Chromatograph Mass Spectrometer (LC-MS). The targeted metabolomics method was modified from a published protocol[22] that used amide HILIC column (XBridge Amide 3.5 μm, 4.6 × 100 mm). The LC method used

two elution solutions; buffer A (95% water and 5% acetonitrile with 20 mM ammonium hydroxide and 20 mM ammonium acetate, pH 9.0) and buffer B (acetonitrile). The 0.25 mL/min LC gradient was started from 0 to 0.1 min, 85% B, 3.5 min, 32% B, 12 min, 2% B, 16.5 min, 2% B, 17–16 min, 85% B. The samples were acquired by a QTRAP 5500+ (AB Sciex) using polarity switching approach which referred from published MRM list containing 297 transitions. The LC-MS/MS peak integration was performed on MultiQuant (AB Sciex) to obtain the metabolomics spreadsheet.

Untargeted lipidomics

The nonpolar lipids were reconstituted using 200 µL of 2-propanol: acetonitrile: water (*v:v:v* 30:65:5). Then 5 µL of reconstituted sample was injected into the LC-MS. The untargeted lipidomics method was modified from a published method[23] that used a C30 column (Acclaim C30, 3 µm, 2.1 × 150 mm). The LC method used two elution solutions; buffer A (60% acetonitrile and 40% water with 0.1% formic acid and 10 mM ammonium formate) and buffer B (90% 2-propanol and 10% acetonitrile with 0.1% formic acid and 10 mM ammonium formate). The 0.2 mL/min LC gradient was started from 0 to 1.5 min, 32% B, 4 min, 45% B, 5 min, 52% B, 8 min, 58% B, 11 min, 66% B, 14 min, 70% B, 18 min, 75% B, 21–25 min, 97% B, 25–32 min 32% B. The samples were acquired by a Orbitrap Exploris 480 (Thermo Fisher Scientific) using polarity switching approach with DDA mode. All the lipidomics .RAW files were processed on *LipidSearch* 4.0 (Thermo Fisher Scientific) for the lipid identification.

Metabolomic and lipidomic data analyses

The metabolomic results were statistically analyzed by MetaboAnalyst 5.0.[24] The lipidomic results were statistically analyzed with LINT-web.[25]

Histology

The SBOT tissues were collected and fixed in 10% neutral formalin overnight within 30 min after the surgeries. After conventional dehydration and paraffin embedding, the blocks were cut into 4 mm of slices for hematoxylin and eosin staining. In detail, samples were dewaxed using Xylene for 20 min twice, 100% ethanol for 5 min twice, 75% ethanol for 5 min, and then rinsing with tap water. Sections were stained with Hematoxylin solution for 3–5 min and then rinsed with tap water. Next, sections were treated with Hematoxylin Differentiation solution and Hematoxylin Scott Tap Bluing, rinsed with tap water, respectively. Sections were dehydrated using 85% ethanol for 5 min and 95% ethanol for 5 min, and then stained with Eosin dye for 5 min. Then sections were dehydrated using 100% ethanol for 5 min three times and Xylene for 5 min twice. Finally, sections were sealed with neutral gum. All the ovarian follicles' images were taken by K-viewer. The sections of tumors were affirmed under 10X low power lens. Ten fields were randomly chosen from 40X high power lens of each sample for immune cell counting. The average cell count was compared between recurrence and non-recurrence group using Student *t*-test.

Statistical analysis

GSEA was performed according to its guideline.[26,27] Kolmogorov–Smirnov test was used for normality analysis. Student *t*-test was used for the metabolomics and lipidomics analysis in this study. Wil-Cox test was used for the RNA-seq analysis.

Role of the funding source

The funders of the study had no role in study design, data collection, data analysis, data interpretation, or writing of the report. All authors had access to the datasets of this study and all authors agreed with the final decision to submit for publication.

Results

Clinical features correlated to recurrence of SBOT

Between Aug 2009 and July 2019, a total of 321 patients were diagnosed with SBOT and received surgical treatment in Obstetrics and Gynecology Hospital of Fudan University. Two patients with invasive implantation were excluded from the analysis. Among the 319 patients, we managed to identify the recurrent conditions of 271 patients. Basic patient information is shown in Table 1. The details of how the study population was defined can be found in the Methods.

Among 271 patients in a median follow-up interval of 77 (12–247) month, 59 (18.5%) of them had recurrence with a median recurrence period of 34 (9–132) months. Though the lymphadenectomy rate is high in this cohort, 73% of it happened before the update of FIGO guideline for lymphadenectomy in 2015. Complete cytoreductive surgery has been done for every patient. Two patients that were treated with FSS developed LGSC. Three patients still carried tumors at the end of follow-up. There were 57 recurrent cases that underwent FSS. For the 198 patients receiving fertility sparing surgery, 69 of them have fertility desire. In total 34 patients were pregnant after surgeries and 38 children were born. The features of these patients are shown in Table 1. Multiple recurrence happened in 17 patients, whose conditions were summarized in **Supplementary Table 2**. No one experience disease-related death. The 5- and 10-years progression free survival (PFS) rate in this cohort was 81.2 and 68.8%.

We further explored the correlation between different clinical indicators and recurrence. Five factors were

Characteristics	Internal Cohort			External Cohort		
	The Whole Set	Patients under follow-up		The whole Set	Patients under follow-up	
		Recurrence *n* = 59	Non-recurrence *n* = 212		Recurrence *n* = 24	Non-recurrence *n* = 59
Median age (year)	34 (15−73)	28 (16−48)	38 (15−73)	35 (14−91)	27 (14−37)	43 (16−91)
Median recurrent month	34 (9−132)			41 (16−129)		
Nullipara	185 (58.0%)	24	135	61 (61.0%)	10	43
Stage						
I	244 (76.5%)	37	207	78 (78.0%)	24	46
II	32 (10.0%)	6	26	5 (5.0%)	0	3
III	41 (12.8%)	16	25	17 (17.0%)	0	10
IV	2 (0.7%)	0	2			
Surgical type						
Fertility preservation						
UOC	63 (19.7%)	17	46	6 (6.0%)	1	4
USO	65 (20.4%)	11	54	14 (14.0%)	2	9
BOC	36 (11.3%)	21	15	13 (13.0%)	9	2
USO+CWR	34 (10.7%)	8	26	25 (25.0%)	12	10
TH+BSO	121 (37.9%)	2	119	42 (42.0%)	0	34
Tumor size (cm, ultrasound)	9.5 (1.8−38.0)	11.0 (3.4−25.1)	9 (1.8−27.6)	9.7 (1.7−42.4)	11.0 (3.9−25.2)	8.9 (1.7−41.0)
Tumor size (cm, pathology)	8.9 (0.5−31.5)	10.2 (0.5−31.5)	8.5 (0.5−29.0)	9.5 (1.5−39.0)	11.5 (4.8−22.0)	9.5 (1.5−39.0)
Exophytic tumor	59 (18.5%)	14	45	29 (29.0%)	8	14
Micropapillary Pattern	38 (11.9%)	15	23	20 (20.0%)	4	12
Microinvasion	30 (9.3%)	7	23	6 (6.0%)	2	3
Peritoneal implantation						
No Biopsy	235 (73.6%)	40	195	84 (84.0%)	19	50
No Implantation	42 (13.2%)	5	37	14 (14.0%)	4	8
Non-invasive implantation	42 (13.2%)	14	28	2 (2.0%)	1	1
Omental implantation						
No Biopsy	186 (58.4%)	34	152	87 (87.0%)	19	52
No Implantation	100 (31.3%)	10	90	11 (11.0%)	5	6
Non-invasive implantation	33 (10.3%)	5	28	2 (2.0%)	0	1
Lymph node metastasis						
No Biopsy	240 (68.0%)	56	184	98 (98.0%)	24	57
No metastasis	71 (28.7%)	2	69	2 (2.0%)	0	2
SBOT metastasis	8 (3.33%)	1	7	0	0	0
Peritoneal cytology						
Unknown	182 (57.1%)	34	119	86 (86.0%)	21	51
Negative	99 (31.0%)	17	69	13 (13.0%)	3	7
Positive	38 (11.9%)	8	24	1 (1.0%)	0	1
Complete surgery						
Yes	35 (11.0%)	8	22	0 (0%)		
No	284 (89.0%)	51	190	100 (100%)	24	59

***Table 1*: General and oncological information of the internal cohort (*n* = 319) and external cohort (*n* = 100).**
UOC: unilateral ovarian cystectomy USO: unilateral salpingo-oophorectomy BOC: bilateral ovarian cystectomy USO+CWR: unilateral salpingo-oophorectomy plus contralateral ovarian wedge resection TH+BSO: total hysterectomy + bilateral salpingo-oophorectomy oophorectomy.

significantly correlated with recurrence (Figure 1A). Among them, micropapillary pattern (Supplementary Figure 2) and advanced stage (Figure 1B) have been discovered as risk factors for the recurrence of SBOT in many other studies including the Denmark study mentioned earlier. Based on our cohort, FSS (Figure 1C, microinvasion (Figure 1D), and lymph nodes invasion (Figure 1E) are indicated as factors related to SBOT recurrence in a Han population. We further evaluated the effects of different FSS types on SBOT recurrence. For unilateral tumors, patients who received USO or UOC had no difference on recurrence risk (Hazard Ratio (HR) = 0.87, 95% confidence interval (CI) 0.32 −2.35, P = 0.78) and fertility outcome

A

Multivariate Cox regression analysis for Fudan Cohort

Characteristics	HR	CI	P-Value
Age	0.99	0.97 - 1.02	0.62
Nullipara	0.95	0.60 - 1.52	0.84
Stage	1.45	1.02 - 2.08	0.04*
UorB	1.64	0.99 - 2.73	0.06
Surgical Type	0.83	0.69 - 1.01	0.06
FSS	2.49	1.33 - 4.64	<0.005**
MP	2.03	1.16 - 3.56	0.01**
MI	2.28	1.05 - 4.98	0.04*
PI	1.09	0.79 - 1.51	0.58
OM	1.34	0.94 - 1.91	0.11
LN	0.51	0.29 - 0.91	0.02*
Cytology	0.99	0.72 - 1.37	0.95
Complete Surgery	0.80	0.37 - 1.73	0.57

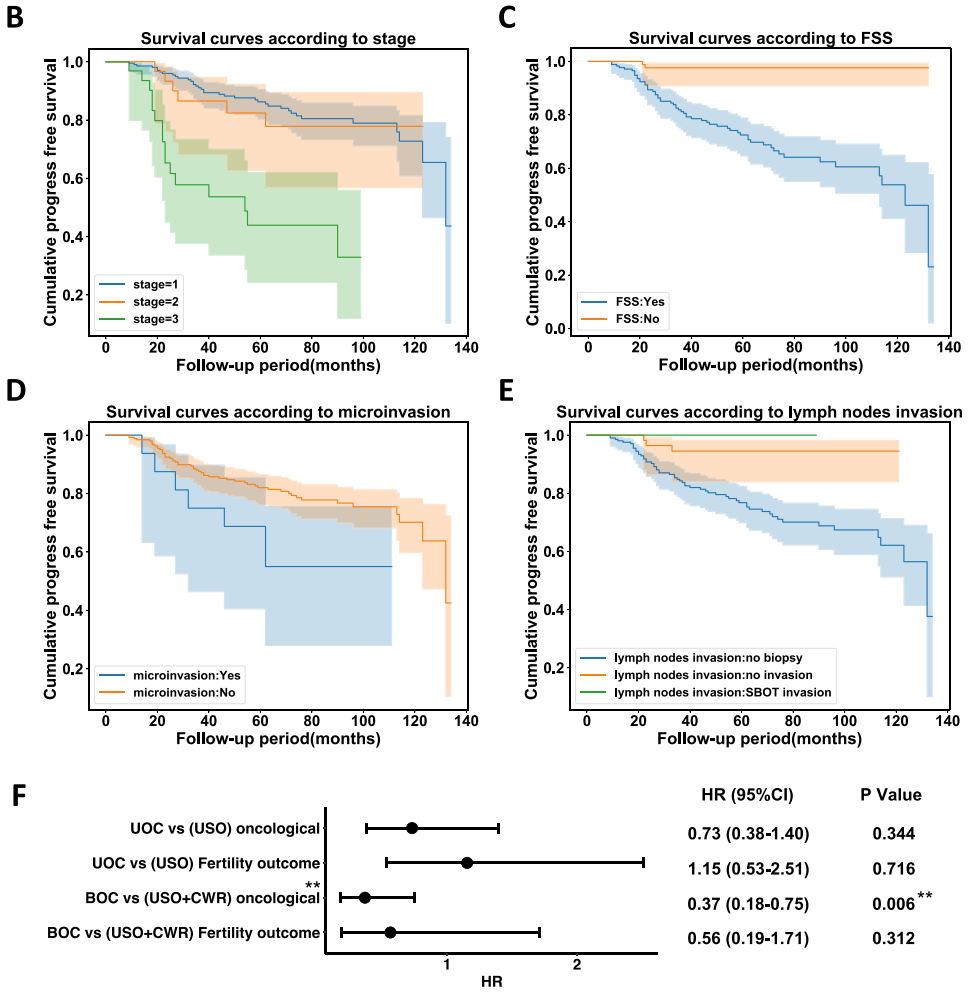

Figure 1. *Identification of risk factors for SBOT recurrence by Multivariate Cox regression*. **A.** Summary for the results of Multivariate Cox regression; **B.** Progress-free survival curves according to stage; **C.** Progress-free survival curves according to FSS; **D.** Progress-free survival curves according to microinvasion; **E.** Progress-free survival curves according to lymph nodes invasion; **F.** Comparison of the effects between different FSS types on clinical outcomes. UorB: unilateral or bilateral tumors; MP: micropapillary patten; MI: microinvasion; OM: omental implantation; LN: lymph nodes invasion; *$p < 0.05$, **$p < 0.01$.

(HR = 1.19,95%CI 0.51−2.82, $P = 0.69$) (Figure 1F). For bilateral tumors, patients received USO+CWR demonstrated lower recurrence risk than BOC (HR = 0.09, 95%CI 0.02−0.38, $P < 0.01$) but no difference in fertility outcome (HR = 0.48, 95%CI 0.13−1.77, $P = 0.27$) (Figure 1F). Notably, the results about complete surgery are limited by its low number in our study and needs to be validated by other studies in future.

A random forest-based prediction tool for the recurrence of SBOT

Identification of patients with a high risk of recurrence is an important way to improve medical care for patients with SBOT. Though several risk factors have been identified, it is a challenge to directly translate these parameters into the prediction of recurrence. Utilizing recent advancements in computational biology, it is possible to establish prediction tools for clinical applications based on features of diseases.[28,29] We therefore tested the fitness of a few computational algorithm, including XGboost, LightGBM, gcForest, and Random Forest Regressor, with the 28 clinical features based on area under the receiver operating characteristics curve (AUC). The details of testing results are summarized in Supplementary Table 3. Random Forest Regressor outperformed other models to achieve the highest numerical AUC (0.999) on internal validation data (Figure 2A and B). Notably, this prediction model achieved excellent predictive power with an AUC of 0.817 on an independent cohort with 100 patients (83 with labels for prediction and 24 recurrences) from Shandong Provincial Hospital from 2009 to 2019 (Figure 2C). These results indicated our computational model can estimate the recurrent risk in patients within the Han population.

For the physicians, one major issue in preventing the broad application such prediction tools is that it is not easy to use these computational algorithms. To this end, we designed a website-based computational tool for SBOT recurrence prediction in a user-friendly style (http://117.25.169.110:1030/). Considering the difficulties associated with collecting information for all 28 parameters, we identified 7 key features which can reach the AUC of 0.990 for the internal cohort and of 0.802 for the external cohort. The features are surgical type, FSS, tumor size (cm, ultrasound), CA199, CA125, age, and white blood cell (WBC). Physicians can simply type in these parameters, or upload a summarized table in the indicated format, to predict the recurrence rate of their patients with SBOT (Figure 2D).

Next-generation sequencing analysis reveals the genetic and transcriptomic features of SBOT recurrence

Twenty-one original SBOT samples were collected during the primary SBOT surgery performed on patients. After following up for 53 (24−78) months, the recurrent conditions of patients were recorded, and the samples were divided into 8 recurrent vs 13 non-recurrent samples. The basic clinical information is summarized in Supplementary Table 4. Firstly, whole genome sequencing (WGS) was performed on these samples to identify common mutations. Unfortunately, no mutations shared by more than three patients were discovered (Supplementary Table 5). These results indicated the genetic diversity of SBOT in a Han population.

Although we did not identify common mutations using WGS, Gene Set Enrichment Analysis (GSEA) revealed genes carrying specific variants in recurrent SBOT are related to important factors for cancer, such as KRAS signaling and immunology (Supplementary Figure 3A). We did observe 1154 genes that were differentially expressed between the recurrent and non-recurrent group via RNA-seq assay (Figure 3A and Supplementary Table 6). Surprisingly, GSEA revealed that different oncogenes were related to either recurrent (*MYC*) and non-recurrent (*KRAS*) SBOT samples (Figure 3B). The negative correlation between recurrent SBOT and KRAS signaling is consistent with the genomic results. The expression of representative genes was further validated by RT-qPCR (Supplementary Figure 3B).

Many clinical studies have revealed the strong positive correlation between KRAS signaling and the outcome of immune therapies. We, therefore, explored the expression of immunological genes in SBOT samples. Consistently, many immune-related genes were downregulated in recurrent SBOT (Figure 3C). The expression of representative genes related to TNFA signaling, IFNA signaling, IFNG signaling, IL6-JAK-STAT3 signaling, and IL2-STAT5 signaling are presented in Figure 3D.

Immune responses to tumor development have been recognized as an important risk factor for the recurrence and prognosis. Thus, we hypothesized that immunological suppression is an important reason for the recurrence of SBOT. Immunological suppression can be induced by decreased infiltration or dysfunction of immune cell in and near tumors. By investigating the histological images of patients with SBOT, we realized that immune cell infiltration is comparable between recurrent and non-recurrent SBOT (Supplementary Figure 3C). So, immune cell dysfunction, and not immune cell number, is likely one of the reasons of recurrent SBOT.

Metabolic regulation of immune cell function in SBOT recurrence

Among many factors capable of regulating immune cell function, metabolites and lipids have been shown to play a particularly important role in tumor immune responses. We firstly measured the changes in metabolites with targeted metabolomics. We found that recurrent and non-recurrent SBOT contains many

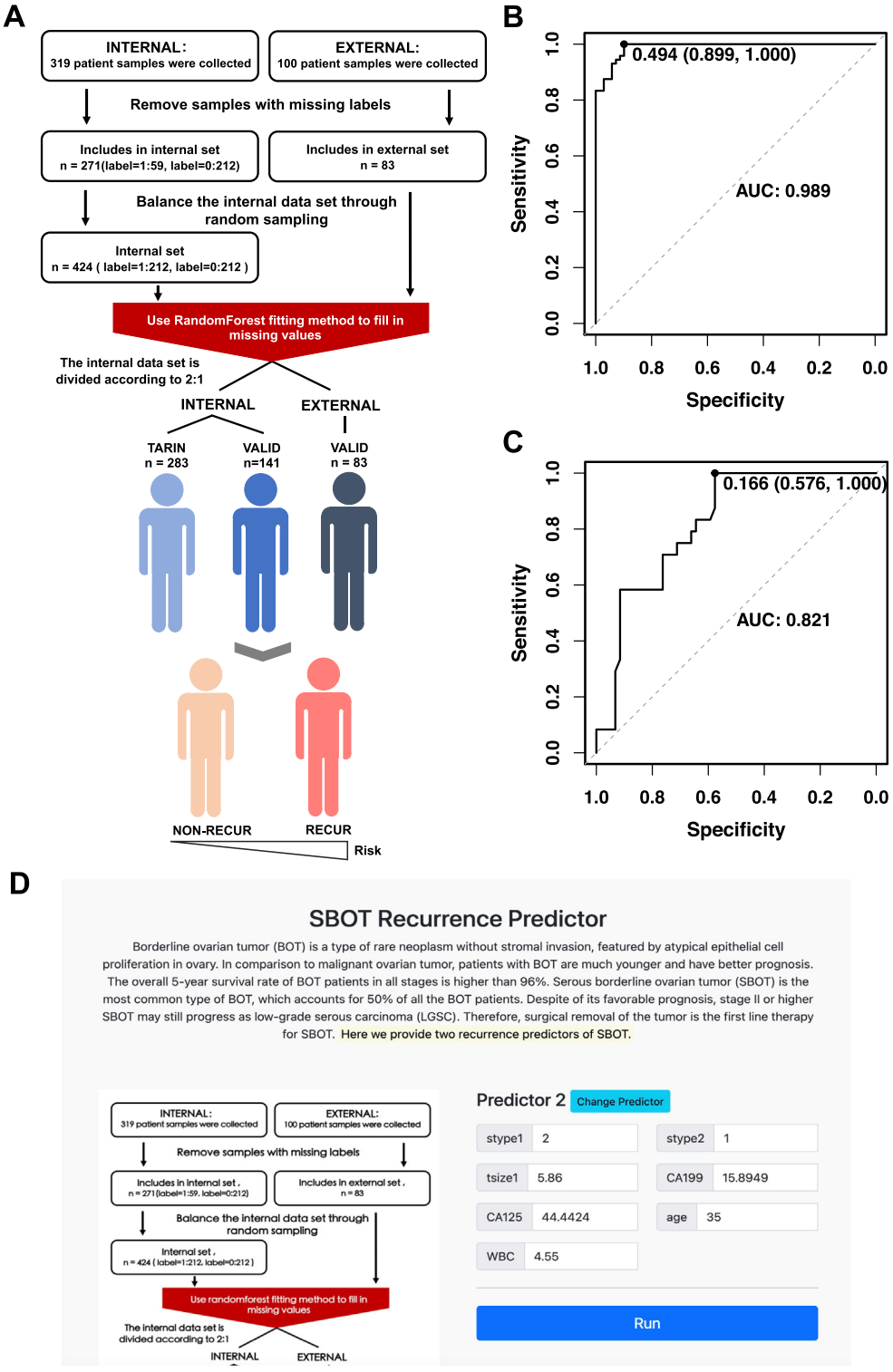

Figure 2. *An online tool to predict SBOT recurrence.* **A.** Establishment of random forest-based prediction tool; **B.** The Receiver Operating Characteristic (ROC) curve of prediction on the internal validation cohort; **C.** The ROC curve of prediction on the external cohort; **D.** The screen shot of the online prediction tool.

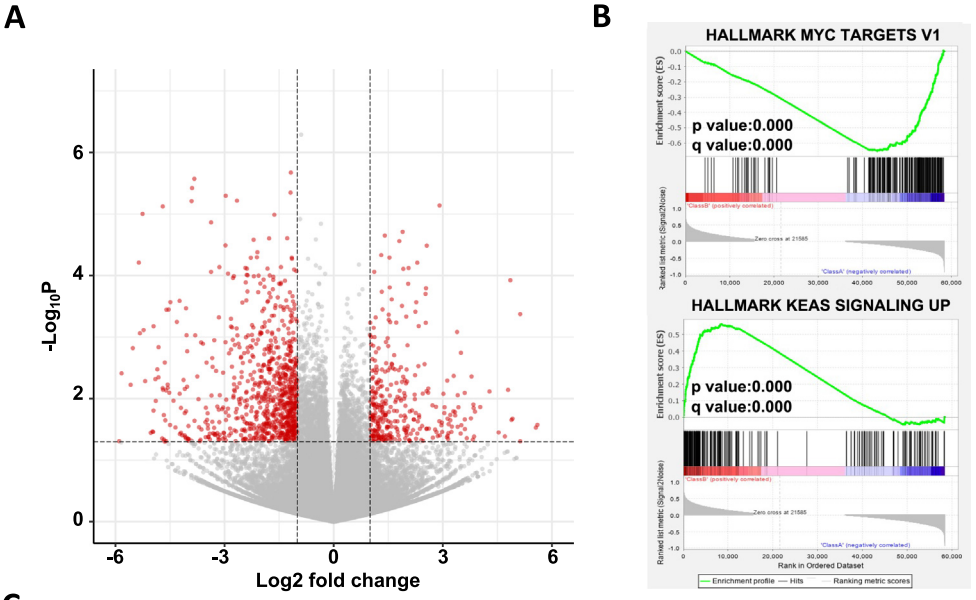

C

The down-regulated signaling of GSEA for Recurrent samples

ITEM	P-Value	Q-value
EPITHELIAL MESENCHYMAL TRANSITION	0.000	0.000
ALLOGRAFT REJECTION	0.000	0.000
TNFA SIGNLING VIA NFKB	0.000	0.000
INFLAMMATORY RESPONSE	0.000	0.000
IL6 JAK STAT3 SIGNALING	0.000	0.000
INTERFERON GAMMA RESPONSE	0.000	0.000
COMPLEMENT	0.000	0.000
KARS SIGNALING UP	0.000	0.000
INTERFERON ALPHA RESPONSE	0.000	0.000

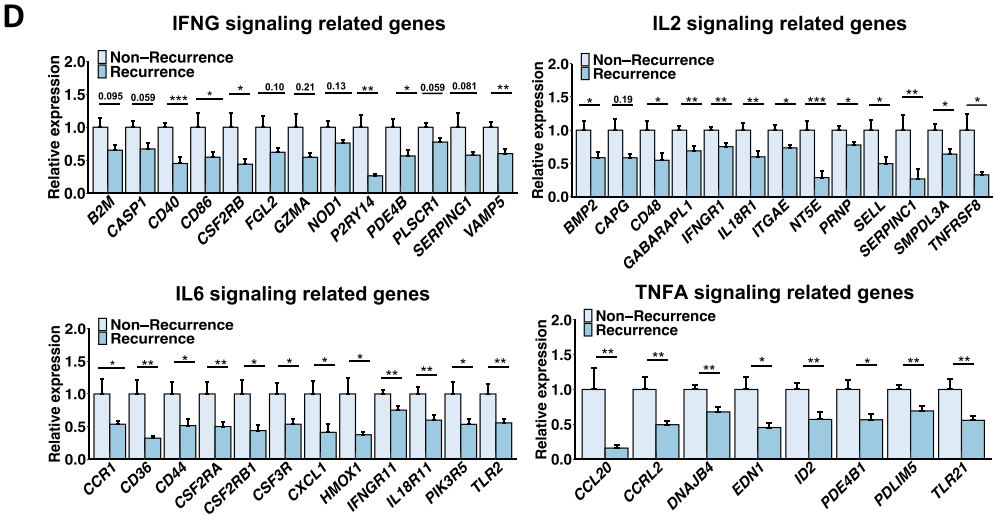

Figure 3. *Transcriptomic features of SBOT recurrence.* A. Significantly changed genes in SBOT recurrence shown on volcano plot; B. Enrichment of significantly changed genes in MYC targets and KRAS signaling by GSEA; C. GSEA enrichment results of down-regulated genes in SBOT recurrence; D. Immunology related genes in SBOT recurrence. *, $p < 0.05$; **, $p < 0.01$; ***, $p < 0.001$.

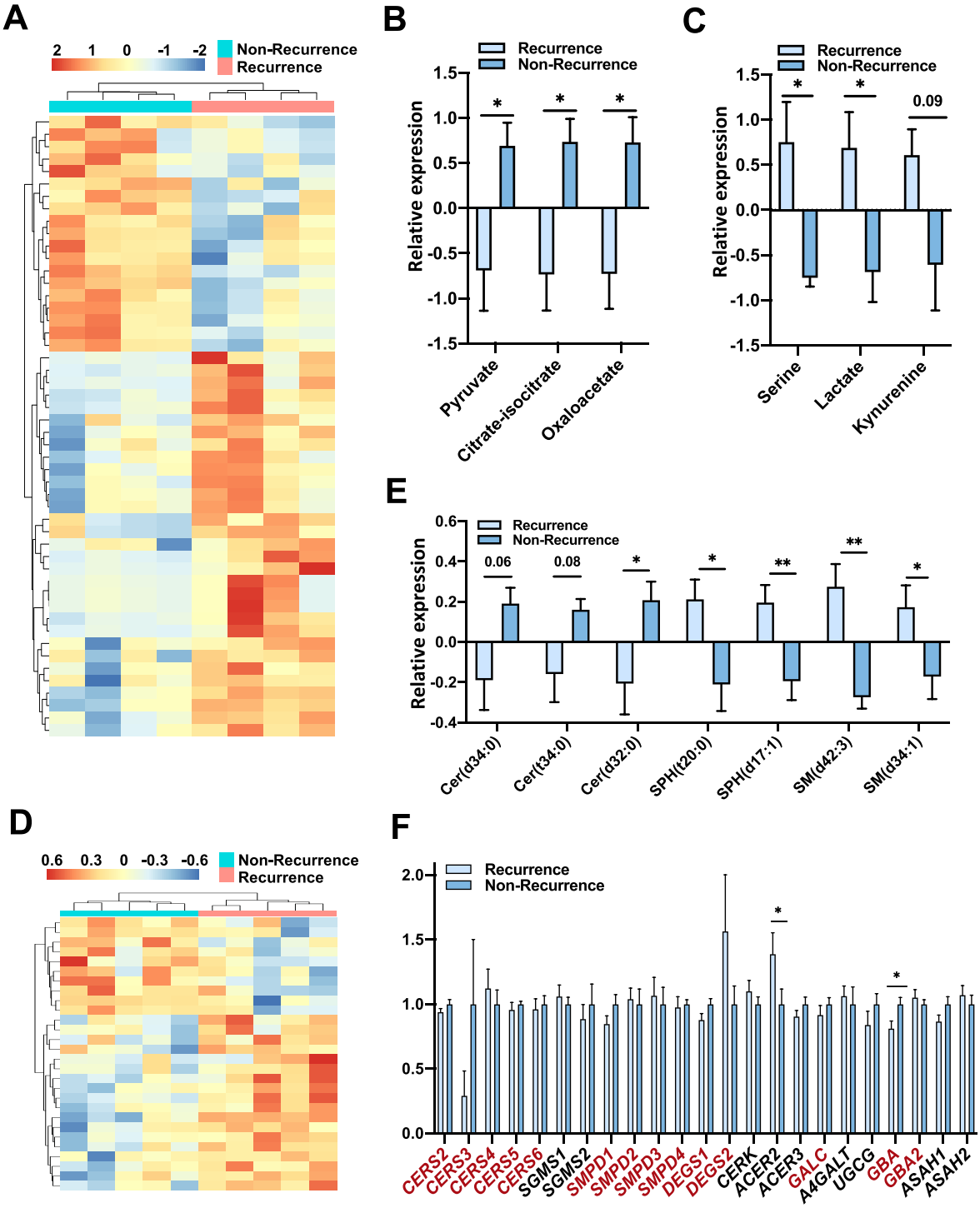

Figure 4. *Metabolic disorders in SBOT recurrence*. A. Heatmap showing the top 75 changed metabolites in SBOT recurrence; B. Representative downregulated metabolites and C. upregulated metabolites in SBOT recurrence; D. Heatmap showing the top 50 changed lipids in SBOT recurrence; E. Downregulation of various ceramides in SBOT recurrence; F. Expression level of genes related to ceramide metabolism. Genes which may upregulate ceramide level were marked in red. *, $p < 0.05$; **, $p < 0.01$.

metabolites with varying abundance (Figure 4A and Supplementary Table 7). The non-recurrent samples contained higher levels of metabolites related to glycolysis and the tricarboxylic acid cycle, such as pyruvate, citrate-isocitrate, and oxaloacetate (Figure 4B). In contrast, recurrent samples contained higher levels of several immunosuppressive metabolites, such as serine, lactate, and kynurenine (Figure 4C).

We also performed untargeted lipidomics on these samples. The recurrent and non-recurrent SBOT samples also contained many lipids with varying abundance (Figure 4D and Supplementary Table 8). Consistently, several immune-related lipids, such as various ceramides, sphingosine, and sphingomyelin, were altered in recurrent SBOT (Figure 4E). By screening the expression of genes regulating sphingolipid metabolism, we identified significant downregulation of *GBA* and upregulation of *ACER2* which may be responsible for changes in ceramide abundance in recurrent SBOT (Figure 4F). Therefore, the changes in immune-related metabolites and lipids may contribute to the immunological suppression observed in recurrent SBOT. Based on its molecular features, we hypothesized that the metabolic changes and the consequent immune suppression are responsible, in part, for disease recurrence in patients with SBOT.

Discussion

To improve the efficacy of therapeutic treatment of SBOT, it is important to identify disease features that are correlated to recurrence. Though the large Denmark study identified non-invasive low-grade serous carcinoma (non-invasive LGSC), bilateral tumor, surface involvement, and invasive implantation as risk factors for progression, this study did not provide a tool to estimate recurrence risk in patients with SBOT. Also, the Denmark study did not comment on the safety and effectiveness of FSS and was lacking in ethnic diversity because most of the patients in the Denmark study were Caucasian.

With a large SBOT cohort in a Han population, we discovered five first-class factors and one second-class factor related to recurrence. The risk factors for recurrence are FSS, advanced stage, micropapillary patten, microinvasion, and lymph nodes invasion.

Microinvasion is a type of stromal invasion that has a controversial correlation to recurrence risk. However, the pathological diagnosis of microinvasion has proven to be complicated, which contains some forms as early stage of destructive stromal invasion. Similar morphological diversity also exists in lymph node invasion, which was not linked to recurrence in a previous SBOT study. Due to the potential correlation of these factors to recurrence, it would be helpful if a more detailed report on microinvasion and lymph node invasion was provided during pathology assessment of tissues.

Although we found FSS to be a risk factor for tumor recurrence, it has been reported that overall prognosis was improved by subsequent surgeries on the recurrent tumor tissue.[30] With consideration to individual patients' wishes for future fertility, it is still feasible for patients with SBOT to receive FSS. Particularly, we found USO+CWR leads to lower recurrence rate than BOC for bilateral tumor. Further studies are needed to validate that USO+CWR is a more suitable FSS for patients with SBOT with bilateral tumor with prospective cohorts.

To better help physicians estimate the prognosis of patients with SBOT, we built a random forest-based online predication tool in a user-friendly format. This tool can predict whether recurrence will happen or not in patients with 7 or 28 key clinical features. The predictive ability of this tool is validated by the study set (AUC = 0.999) and an independent set (AUC = 0.817), even though the prognosis is significantly different between these two sets (**Supplementary Figure 4**). This tool is fully free and open-source. Any physicians with access to the internet can use this tool directly or revise it to better fit their context.

To explore the mechanisms involved in SBOT recurrence, we also investigated molecular features associated with SBOT recurrence using a multi-omics assay. The next-generation sequencing-based assays unveiled that KRAS-related immunological suppression occurs in recurrent SBOT tissues, which may be induced by changes to immune-related metabolites and lipids in the tumor. Nowadays, the therapeutic effects of several immunotherapies on ovarian tumor have been confirmed by clinical trials. In addition, a few metabolic therapies have been developed to facilitate immunotherapies. Our findings suggest the immunotherapies, in combination with metabolic therapies, have the potential to be applied on patients with SBOT to improve their prognosis.

Because the average income of peoples living in Shanghai and Shandong is higher, the results of our clinical study may have bias and needs to be validated by other studies performed by different clinics in future. Our clinical study is also limited by the fact that only Chinese patients are included. We have observed the non-random missing data, which was enriched in HE4, CA199 and AST, in our study. The sensitivity analysis suggested the dropout of these data had no significant effects on the model performance. But it is possible that a better prediction model can be established with complete dataset.

The mechanistic studies were certainly limited by the low number of samples, though we have used all the available SBOT samples in Obstetrics and Gynecology Hospital of Fudan University since 2014. The biological conclusions derived from current study need to be validated by other investigators working on SBOT in the future. We also cannot identify common mutations

that might be shared by a large portion of patients with SBOT with similar prognoses. However, the novel recurrence-related factors we found, the prediction tool we established, and the immunological suppression features we identified will improve the clinical practice and mechanistic studies of SBOT recurrence.

Funding

JL was funded by MOST 2020YFA0803600, 2018YFA0801300, NSFC 32,071,138, and SKLGE-2118 to Jin Li; JY was funded by the Initial Project for Young and Middle-aged Medical Talents of Wuhan City, Hubei Province ([2014] 41); HH was funded by MOST 2019YFA0801900 and 2020YF1402600 to He Huang; JS was funded by NSFC 22,104,080; CG was funded by Natural Science Foundation of Shanghai 20ZR1408800 and NSFC82171633; BL was funded by Natural Science Foundation of Shanghai 19ZR1406800.

Contributors

Conceptualization, ZL, FL, TL, JS, CG, JL; Investigation, ZL, FL, TL, JW, CL, GL, JL; Analysis, ZL, FL, JS, JL; Writing, ZL, FL, TL, JW, CL, GL, BL, MP, SF, JY, HH, JS, CG, JL; Funding Acquisition, HH, JY, CG, JS, BL, JL; Supervision, JS, CG, JL. Dr. Jin Li, Dr. Chao Gu and Dr. Jia Song have accessed and verified the data. All authors confirm that they had full access to all the data in the study and accept responsibility to submit for publication. All the authors promise the accuracy and completeness of the data. All authors participated the revision and approved the final version of manuscript.

Data sharing statement

The source code for the prediction tool is available at https://github.com/songjiajia2018/SBOT. The original data of this study are available on request from the corresponding author Dr. Jin Li (li_jin_lifescience@fudan.edu.cn).

Declaration of interests

The authors declare no potential conflicts of interest.

Supplementary materials

Supplementary material associated with this article can be found in the online version at doi:10.1016/j.eclinm.2022.101377.

References

1 Fischerova D, Zikan M, Dundr P, Cibula D. Diagnosis, treatment, and follow-up of borderline ovarian tumors. *Oncologist*. 2012;17(12):1515–1533.

2 Morice P, Uzan C, Fauvet R, Gouy S, Duvillard P, Darai E. Borderline ovarian tumour: pathological diagnostic dilemma and risk factors for invasive or lethal recurrence. *Lancet Oncol*. 2012;13(3):e103–e115.

3 Hauptmann S, Friedrich K, Redline R, Avril S. Ovarian borderline tumors in the 2014 WHO classification: evolving concepts and diagnostic criteria. *Virchows Arch*. 2017;470(2):125–142.

4 Prat J. Pathology of borderline and invasive cancers. *Best Pract Res Clin Obstet Gynaecol*. 2017;41:15–30.

5 Uzan C, Muller E, Kane A, et al. Fertility sparing treatment of recurrent stage I serous borderline ovarian tumours. *Hum Reprod*. 2013;28(12):3222–3226.

6 Chen RF, Li J, Zhu TT, Yu HL, Lu X. Fertility-sparing surgery for young patients with borderline ovarian tumors (BOTs): single institution experience. *J Ovarian Res*. 2016;9:16.

7 Helpman L, Yaniv A, Beiner ME, et al. Fertility preservation in women with borderline ovarian tumors - how does it impact disease outcome? A cohort study. *Acta Obstet Gynecol Scand*. 2017;96(11):1300–1306.

8 Morice P, Camatte S, El Hassan J, Pautier P, Duvillard P, Castaigne D. Clinical outcomes and fertility after conservative treatment of ovarian borderline tumors. *Fertil Steril*. 2001;75(1):92–96.

9 Camatte S, Morice P, Pautier P, Atallah D, Duvillard P, Castaigne D. Fertility results after conservative treatment of advanced stage serous borderline tumour of the ovary. *Bjog*. 2002;109(4):376–380.

10 Uzan C, Kane A, Rey A, Gouy S, Duvillard P, Morice P. Outcomes after conservative treatment of advanced-stage serous borderline tumors of the ovary. *Ann Oncol*. 2010;21(1):55–60.

11 Song T, Choi CH, Kim HJ, et al. Oncologic and reproductive outcomes in patients with advanced-stage borderline ovarian tumors. *Eur J Obstet Gynecol Reprod Biol*. 2011;156(2):204–208.

12 Jia SZ, Xiang Y, Yang JJ, Shi JH, Jia CW, Leng JH. Oncofertility outcomes after fertility-sparing treatment of bilateral serous borderline ovarian tumors: results of a large retrospective study. *Hum Reprod*. 2020;35(2):328–339.

13 Vo TM, Duong KA, Tran LT, Bui TC. Recurrence rate and associated factors of borderline ovarian tumors in the south of Vietnam. *J Obstet Gynaecol Res*. 2019;45(10):2055–2061.

14 Hannibal CG, Vang R, Junge J, et al. A nationwide study of serous "borderline" ovarian tumors in Denmark 1978-2002: centralized pathology review and overall survival compared with the general population. *Gynecol Oncol*. 2014;134(2):267–273.

15 Ren J, Peng Z, Yang K. A clinicopathologic multivariate analysis affecting recurrence of borderline ovarian tumors. *Gynecol Oncol*. 2008;110(2):162–167.

16 El-Balat A, Schmeil I, Gasimli K, et al. Claudin-1 is linked to presence of implants and micropapillary pattern in serous borderline epithelial tumours of the ovary. *J Clin Pathol*. 2018;71(12):1060–1064.

17 Sadłecki P, Grabiec M, Grzanka D, Jóźwicki J, Antosik P, Walentowicz-Sadłecka M. Expression of zinc finger transcription factors (ZNF143 and ZNF281) in serous borderline ovarian tumors and low-grade ovarian cancers. *J Ovarian Res*. 2019;12(1):23.

18 Armstrong DK, Alvarez RD, Bakkum-Gamez JN, et al. NCCN guidelines insights: ovarian cancer, version 1.2019. *J Natl Compr Canc Netw*. 2019;17(8):896–909.

19 Bolger AM, Lohse M, Usadel B. Trimmomatic: a flexible trimmer for Illumina sequence data. *Bioinformatics*. 2014;30(15):2114–2120.

20 Sahraeian SME, Mohiyuddin M, Sebra R, et al. Gaining comprehensive biological insight into the transcriptome by performing a broad-spectrum RNA-seq analysis. *Nat Commun*. 2017;8(1):59.

21 Huang H, Yuan M, Seitzer P, Ludwigsen S, Asara JM. IsoSearch: an untargeted and unbiased metabolite and lipid isotopomer tracing strategy from HR-LC-MS/MS datasets. *Methods Protoc*. 2020;3(3).

22 Yuan M, Breitkopf SB, Yang X, Asara JM. A positive/negative ion-switching, targeted mass spectrometry-based metabolomics platform for bodily fluids, cells, and fresh and fixed tissue. *Nat Protoc*. 2012;7(5):872–881.

23 Breitkopf SB, Ricoult SJH, Yuan M, et al. A relative quantitative positive/negative ion switching method for untargeted lipidomics via high resolution LC-MS/MS from any biological source. *Metabolomics*. 2017;13(3):1–21.

24 Pang Z, Chong J, Li S, Xia J. MetaboAnalystR 3.0: toward an optimized workflow for global metabolomics. *Metabolites*. 2020;10(5).

25 Li FS, Song J, Zhang YK, et al. LINT-Web: a web-based lipidomic data mining tool using intra-omic integrative correlation strategy. *Small Methods*. 2021;5(9).

26 Mootha VK, Lindgren CM, Eriksson KF, et al. PGC-1alpha-responsive genes involved in oxidative phosphorylation are coordinately downregulated in human diabetes. *Nat Genet*. 2003;34(3):267–273.

27 Subramanian A, Tamayo P, Mootha VK, et al. Gene set enrichment analysis: a knowledge-based approach for interpreting genome-wide expression profiles. *Proc Natl Acad Sci U.S.A.* 2005;102 (43):15545–15550.
28 Zhao S, Nicolle R, Augustin J, et al. Prognostic relevance of pancreatic adenocarcinoma whole-tumor transcriptomic subtypes and components. *Clin Cancer Res.* 2021:6491–6499.
29 McIntosh C, Conroy L, Tjong MC, et al. Clinical integration of machine learning for curative-intent radiation treatment of patients with prostate cancer. *Nat Med.* 2021;27(6):999–1005.
30 Fang C, Zhao L, Chen X, Yu A, Xia L, Zhang P. The impact of clinicopathologic and surgical factors on relapse and pregnancy in young patients (≤40 years old) with borderline ovarian tumors. *BMC Cancer.* 2018;18(1):1147.